

Electro-thermal Aspects in Carbon based Interconnects

Rekha Verma, Sitangshu Bhattacharya and Santanu Mahapatra

Nanoscale Device Research Laboratory
Department of Electronic Systems Engineering
Indian Institute of Science, Bangalore 560 012, India
Email: rekha.verma26@gmail.com, isbsin@yahoo.co.in, santanu@cedt.iisc.ernet.in

ABSTRACT

In this work, we analyze self-heating in suspended single layer graphene (SLG) by using temperature dependent flexural phonon (ZA) dominated thermal conductivity (κ) for both isotopically pure and impure cases on the basis of second order three phonon Umklapp, mass difference and edge roughness scatterings. This is followed by the extraction of temperature dependent electrical resistance ($R(T)$) of SLG sheet as a result of Joule-heating along the sheet when a constant current is passed through it. It is found that pure SLG sheet leads to a low rising in temperature. However, with the addition of isotopic impurities, κ falls down as a result of mass difference scattering which significantly rises the temperature along the sheet. The methodologies as presented here can be used for obtaining an accurate analysis of the temperature profile along the SLG based interconnects and hence to predict the hot-spot location within the chip.

Keywords: Joule heating, single layer graphene, thermal conductivity, flexural phonon.

1 INTRODUCTION

Tremendous rise in Joule-heating in conventional Cu/Al interconnects inside modern ICs due to continuous down-scaling has led down ITRS [1] to ensure on material alternatives that surpasses their break-down current density and thermal conductivity (κ) (10^6 A cm^{-2} and 401 Wm $^{-1}$ K $^{-1}$ and 237 Wm $^{-1}$ K $^{-1}$ at 300 K) beyond room temperature (RT). In recent years, carbon nanomaterials, like metallic single-walled carbon nanotubes (SWCNTs) and single layer graphene (SLG), have been found to possess very high RT mobility, break-down current density and κ (of the order of $20,000$ $cm^2V^{-1}s^{-1}$ to $2,00,000$ $cm^2V^{-1}s^{-1}$, 10^8 - 10^9 Acm $^{-2}$ and 600 - 7000 W $^{-1}$ K $^{-1}$, respectively [2,3]). However, there is a tremendous controversy that whether these phenomena are due to LA/TA [2,3,4,5,6] or flexural (ZA) phonon values [7,8,9]. A fundamental physics-based model for electro-thermal resistances is thus strongly needed in order to estimate the Joule heating/temperature rise and hot-spot location, cross-talks, and electro-migration effects in bundles and layers of these materials for optimizing power dissipation calculations and providing a model of simple carbon based IC prototype. In this work, we analyze self-heating in suspended SLG by using temperature dependent ZA dominated κ [11]

for both isotopically pure and impure on the basis of second order three phonon Umklapp, mass difference (MD) and edge roughness scatterings. It is demonstrated that a quadratic ZA phonon exhibits a T $^{-2}$ law beyond room temperature on κ , whereas below room temperature the trend matches with the experimentally established T $^{1.5}$ behaviour [2,3,10]. This is followed by the extraction of $R(T)$ as a result of Joule-heating along the sheet when a constant current is passed through it [12]. By incorporating the physics based analytical models of $R(T)$ and κ into Joule-heating equation, one can accurately estimate the temperature distribution along the SLG sheet. The temperature profile along the metallic SWCNTs has already been reported by the authors [13] and in the present work we restrict our analysis to the SLG sheet only. It is found that pure SLG sheet leads to a low rising in temperature. However, with the addition of isotopic impurities, κ goes down due to increased MD scattering rate which significantly rises the temperature along the sheet. The methodologies as presented here can be used for obtaining an accurate analysis of the temperature profile along the SLG sheet and hence to predict the hot-spot location, thermal cross-talk, electromigration effects within the chip using carbon as interconnect material.

2 MODEL DEVELOPMENT AND DISCUSSIONS

The realization of the second order three phonon Umklapp scattering rate $\frac{1}{\tau_U} = \frac{32}{27}|\gamma_{ZA}|^4 \left(\frac{k_B T}{M(\partial\omega_q/\partial q)} \right)^2 \omega_B$ [14], the MD scattering rate $\frac{1}{\tau_I} = \frac{1}{4}S_0\Gamma_m \frac{q\omega_q^2}{(\partial\omega_q/\partial q)}$ [14] and the frequency-dependent edge-roughness scattering rate $\frac{1}{\tau_E} = \frac{\sqrt{\pi}}{2F\sqrt{LW}} \left(\frac{\partial\omega_q}{\partial q} \right)$ [14] in SLG leads to the resultant scattering rate (τ_R^{-1}) by Matthiessen's rule: $\tau_R^{-1} = \tau_U^{-1} + \tau_M^{-1} + \tau_E^{-1}$. The parameters $|\gamma_{ZA}|$, ω_B , M , F , Γ_m , $\partial\omega_q/\partial q$, S_0 are the Gruneisen parameter, phonon branch frequency at the zone boundary, mass of the carbon atom, form factor, strength of isotopic impurity, the ZA phonon velocity where q is the ZA phonon vector and the cross-section area per one atom ($= \delta \times r_0$) where $r_0 = 0.14$ nm is the carbon-carbon distance and $\delta=0.335$ nm is the layer thickness of an SLG) respectively. T , L , and W are the temperature, length and width of the suspended SLG respectively. The flexural phonon dispersion relation thus can be written as $\omega_q = \alpha q^2$ in which $\alpha = \sqrt{\frac{\kappa_0}{\rho_0}} \approx 4.6 \times 10^{-7}$ m $^2s^{-1}$ denotes the ZA

phonon diffusion constant [14,15].

We start with the expression of the steady-state Joule-heating equation with a temperature dependent thermal conductivity along the suspended SLG sheet length $-L/2 < x < L/2$ [12] and assuming the contacts to be ideal

$$A\nabla(\kappa\nabla T) + p = 0 \quad (1)$$

where $A = \delta W$ is the cross-sectional area, $p = i_D^2 R(T)/L$ in which i_D is the constant current flowing from left to right contact, $R(T)$ is the linearized Boltzman temperature dependent electrical resistance of the SLG sheet and can be written as [12]

$$R(T) = \frac{\pi\hbar^2}{q^2 E_F} \frac{1}{\tau} \quad (2)$$

in which $\frac{1}{\tau}$ is the resultant scattering rate due to in-plane and flexural phonons and is given by Matthiessen's rule as $\frac{1}{\tau} = \frac{1}{\tau_{inplane}} + \frac{1}{\tau_{flexural}}$ where [14]

$$\frac{1}{\tau_{inplane}} \approx \left[\frac{g^2}{2v_L^2} + \frac{\hbar^2 v_F^2 \beta^2}{4a^2} \left(\frac{1}{v_L^2} + \frac{1}{v_T^2} \right) \right] \frac{E_F}{2\rho\hbar^3 v_F^2} k_B T \quad (3)$$

and

$$\frac{1}{\tau_{flexural}} \approx \left(\frac{g^2}{2} + \frac{\hbar^2 v_F^2 \beta^2}{4a^2} \right) \frac{(k_B T)^2}{64\pi\hbar\zeta^2 E_F} \ln \left(\frac{k_B T}{\hbar\omega_c} \right) \quad (4)$$

Here, k_B is the Boltzmann's constant, $g \approx 3$ eV is the screened deformation potential constant, $\beta \approx 2-3$, $\zeta=1$ eV is the bending rigidity, $a = 1.4\text{\AA}$ is the distance between nearest carbon atoms, $\rho = 7.6 \times 10^{-7} \text{ Kg m}^{-2}$ is the mass density, $v_L = 2.1 \times 10^4$ m/s and $v_T = 1.4 \times 10^4$ m/s are the longitudinal and transverse sound velocities respectively [16]. It has been assumed that the Bloch-Gruneisen temperature ($T_{BG} = 57, 38$ and 0.1K) is far less than the room temperature for longitudinal, transverse and flexural phonons at carrier concentration $n_{2D}=10^{12} \text{ cm}^{-2}$ respectively and the domination of the absorption or emission of two phonons for $T \gg T_{BG}$. It can be seen from Fig. 1 that the analytical model of $R(T)$ agrees well with the available experimental data [17] with sheet dimensions as $L=1 \mu\text{m}$ and $W=1.5 \mu\text{m}$, carrier degeneracy $n_{2D}=10^{12} \text{ cm}^{-2}$ and varying current density ranging from $0.2-1.96$ mA. The detailed physics based analytical model to find out $R(T)$ is reported by the authors in [12].

The ZA phonon mode dominated diffusive thermal conductivity of an SLG sheet can mathematically be written as [18]

$$\kappa = \frac{1}{4\pi\delta k_B T^2} \int_{q=0}^{q_{max}} \left(\frac{\partial\omega_q}{\partial q} \right)^2 (\hbar\omega_q)^2 \tau_q \frac{q e^{\frac{\hbar\omega_q}{k_B T}}}{\left(e^{\frac{\hbar\omega_q}{k_B T}} - 1 \right)^2} dq \quad (5)$$

This leads to the expression of κ at lower temperature (κ_{low}) in an isotopically pure SLG as

$$\kappa_{low} = \left(\frac{Fk_B}{2\delta} \right) \left(\frac{LW}{\alpha} \right)^{\frac{1}{2}} \left(\frac{k_B T}{\pi\hbar} \right)^{\frac{3}{2}} \left[\int_0^{\frac{\theta}{T}} \frac{\xi^{\frac{5}{2}} e^\xi}{(e^\xi - 1)^2} d\xi \right] \quad (6)$$

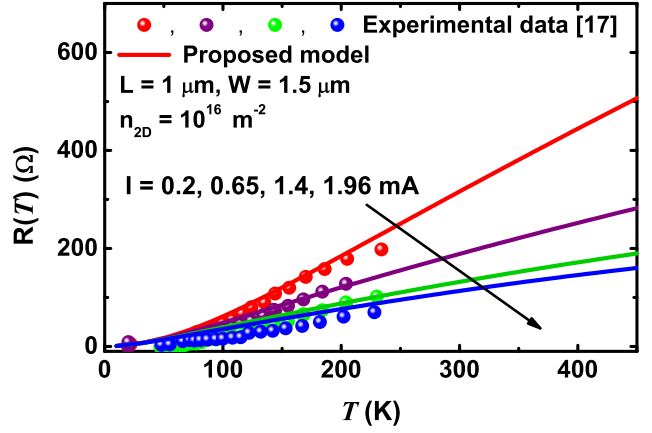


Figure 1: Electrical resistance as a function of temperature for doped SLG at various current levels. The solid lines corresponds to the proposed model and symbols are the experimental data from [17].

The last factor in the parenthesis is generally known as Debye integral of order $5/2$. It can be shown that in the lower temperature regime where the upper integral limit tends to infinity, this $5/2$ order Debye integral converges to a numerical constant value 4.58 . However, at higher temperature regime, (5) converges to

$$\kappa_{high} = \left(\frac{k_B^3}{2\pi\delta} \right) \left(\frac{T}{\hbar} \right)^2 \left[\int_0^{\frac{\theta}{T}} \left(\frac{\xi^3}{B + C\xi^4} \right) \frac{\xi^2 e^\xi}{(e^\xi - 1)^2} d\xi \right] \quad (7)$$

In the absence of isotope density, (7) converges to

$$\kappa_{high} = \left(\frac{27}{16\pi\delta} \right) \left(\frac{k_B}{\hbar} \right)^3 \left(\frac{M\alpha}{|\gamma_{ZA}|^2} \right)^2 \left(\frac{\theta^4}{\hbar\omega_B} \right) \left(\frac{1}{T^2} \right) \quad (8)$$

whereas in the presence of heavy isotopic concentration, (7) approaches

$$\kappa_{high} = \left(\frac{k_B \alpha}{\pi\delta S_0 \Gamma_m} \right) \ln \left| \zeta \frac{\theta^4}{T^2} \right| \quad (9)$$

in which $\zeta = \left(\frac{27S_0 \Gamma_m \alpha}{16\omega_B} \right) \left(\frac{k_B M}{\hbar^2 |\gamma_{ZA}|^2} \right)^2$. While deriving equations (7)-(9), we have assumed that the function $\xi^2 e^\xi / (e^\xi - 1)^2$ at high temperatures approaches unity. Thus, the total thermal conductivity can finally be modelled for both the aforementioned cases as

$$\kappa^{-1} = \kappa_{low}^{-1} + \kappa_{high}^{-1} \quad (10)$$

for a wide range of temperature. Fig. 2 exhibits κ as a function of T for suspended SLG over a rectangular trench of various dimensions. The analytical model is shown by solid and dotted lines and is in well agreement with the experimental data [2,3] shown by symbols.

The use of these physics based thermal conductivity and electrical resistance models in (1) and solving it numerically by choosing appropriate boundary conditions i.e., $T(-L/2) = T_L$ and $T(L/2) = T_H$, where T_L and T_H are the temperatures at two end point contacts, the solution to (1) leads to the temperature distribution along

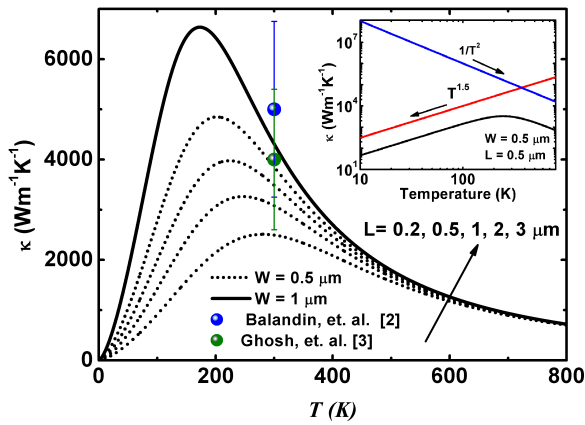


Figure 2: κ as function of temperature for suspended SLG over a rectangular trench of various dimensions. The solid and dotted curves corresponds to the present analytical model for different widths. The symbols are the experimental data from [2] and [3]. The inset exhibits the same plot showing the temperature dependency of κ at low T and high T .

the length of an isotopically pure and impure SLG sheet. The analytical solution to (1) can be done by referring to the authors previous work done for metallic SWCNT [13]. The temperature profile along the SLG sheet for

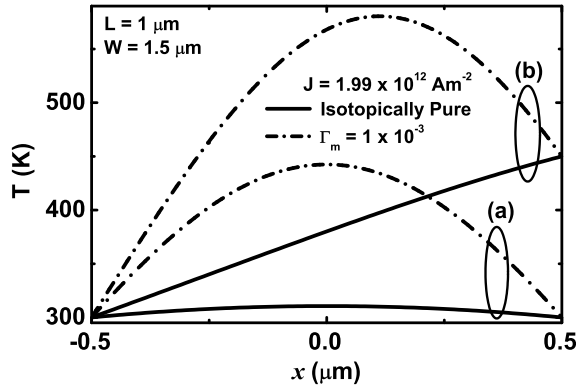


Figure 3: T as a function of x for both isotopically pure and impure cases and for a constant current of $J=1.99 \times 10^{12} \text{ Am}^{-2}$ and sheet dimensions of $L=1 \mu\text{m}$ and $W=1.5 \mu\text{m}$ when (a) both the contacts are at 300 K and (b) both one contact is at 300 K and other is at 450 K.

both the isotopically pure and impure cases has been plotted when both the ends are at same temperature at 300 K, and when one end is at 300 K and the other at 450 K as shown in the groups (a) and (b) respectively in Fig. 3. It can be understood from Fig. 3 that there is a significant difference in temperature profile when compare the pure case with an impure one. The temperature rise in case of pure SLG sheet is lower as compared to the identical case when the sheet is isotopically impure. This is due to the fact that as the form factor (Γ_m) increases, the thermal conductivity goes down

as a result of increased mass-difference scattering rate which in turn increases the temperature along the sheet. The maximum temperature is at the centre of the sheet length when both the ends are kept at 300 K and the temperature difference is about 150 K between isotopically pure and impure sheets in this case. When one end is at 300 K and other end is at 450 K, the maximum temperature point shifts towards the higher T end point contact and there is a significant rise in T when compare the pure case with an impure one. Fig. 4 exhibits

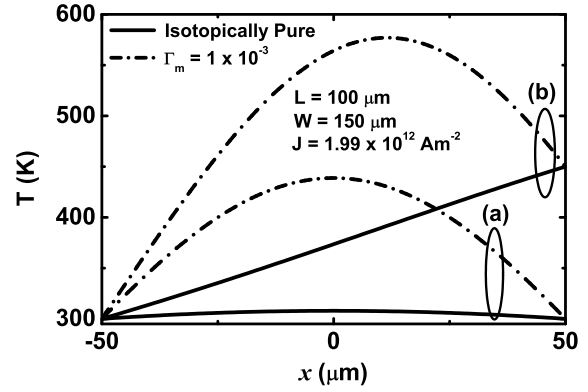


Figure 4: T as a function of x for both isotopically pure and impure cases and for a constant current of $J=1.99 \times 10^{12} \text{ Am}^{-2}$ and sheet dimensions of $L=100 \mu\text{m}$ and $W=150 \mu\text{m}$ when (a) both the contacts are at 300 K and (b) both one contact is at 300 K and other is at 450 K.

the temperature profile for the identical cases of Fig. 3 but for sheet dimensions of $L=100 \mu\text{m}$ and $W=150 \mu\text{m}$. The temperature rise goes slightly lower when the sheet dimensions are increased. The reason for decrease in T is that the thermal conductivity increases with the sheet length and hence makes T to go down. However, there is no such significant decrease in the temperature profile when the sheet dimensions are extremely large. The dependence of the temperature profile on the form factor is exhibited in Fig. 5, for a sheet dimensions of $L=1000 \mu\text{m}$ and $W=1500 \mu\text{m}$. It is demonstrated that with the decrease in magnitude of the form factor, or in other words, with the increase in the purity of the sheet, the temperature rise also decreases. This is highly expected in this case since, a decrease in Γ_m indicates lesser mass-difference scattering. This lowering of the MD scattering increases sharply the thermal conductivity of the sheet, which further lowers down the overall rise in temperature. As Γ_m decreases, all the curves in Fig. 5 for all the solutions tend to merge to their corresponding saturation value of the pure SLG sheet under identical conditions.

3 CONCLUSIONS

Using a flexural phonon dominated temperature dependent thermal conductivity model and temperature

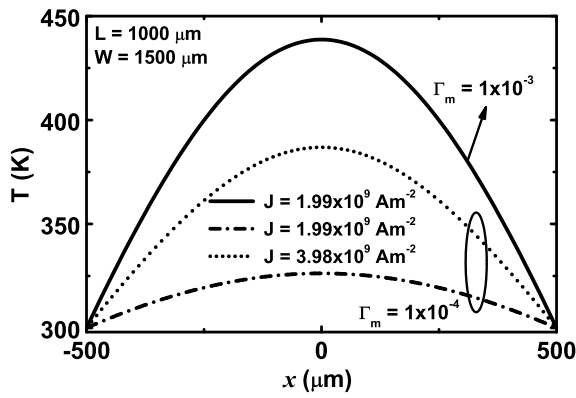


Figure 5: T as a function of x for both isotopically pure and impure cases for sheet dimensions of $L=1000 \mu\text{m}$ and $W=1500 \mu\text{m}$ when both the contacts are at 300 K and for varying current density and form factor (Γ_m).

dependent electrical resistance model, the present study addresses a numerical solution of Joule-heating equation in SLGs. The effect of mass difference scattering has also been introduced for a complete electro-thermal analysis of isotopically impure graphene sheet for more realistic case. It has been found that increase in the form factor, the mass difference scattering severely increases the temperature rise along the length of the sheet. The work as presented here can be put forward for obtaining a fairly well estimation of the temperature profile in carbon based interconnects and hence to predict the hot-spots, electromigration, thermal cross-talks in modern ICs with carbon as interconnect material.

REFERENCES

[1] International Technology Roadmap for Semiconductors, Available Online at: http://www.itrs.net/Links/2009ITRS/2009_Chapters2009Tables/2009Interconnect.pdf.

[2] A. A. Balandin, S. Ghosh, W. Bao, I. Calizo, D. Teweldebrhan, F. Miao and C. N. Lau, "Superior Thermal Conductivity of Single-Layer Graphene", *Nano Lett.*, vol.8, pp. 902-907, (2008).

[3] S. Ghosh, I. Calizo, D. Teweldebrhan, E. P. Pokatilov, D. L. Nika, A. A. Balandin, W. Bao, F. Miao, and C. N. Lau, "Extremely high thermal conductivity of graphene: Prospects for thermal management applications in nanoelectronic circuits", *Appl. Phys. Lett.*, vol.92, pp. 151911 (1)-(3), (2008).

[4] D. L. Nika, E. P. Pokatilov, A. S. Askerov, and A. A. Balandin, "Phonon thermal conduction in graphene: Role of Umklapp and edge roughness scattering", *Phys. Rev. B*, vol.79, pp. 155413 (1)-(12), (2009).

[5] S. Ghosh, W. Bao, D. L. Nika, S. Subrina, E. P. Pokatilov, C. N. Lau and A. A. Balandin, "Dimensional crossover of thermal transport in few-layer graphene", *Nature Mat.*, vol.9, pp. 555-558, (2010).

[6] S. Ghosh, Q. Wu, C. Mishra, J. Kang, H. Zhang, K. Cho, W. Cai, A. A. Balandin and R. S. Ruoff, "Thermal conductivity of isotopically modified graphene", *Nature Mat.*, vol.11, pp. 203-207, (2012).

[7] E. Mariani and F. von Oppen, "Flexural phonons in free-standing graphene", *Phys. Rev. Lett.*, vol. 100, pp. 113401(1)-(4), (2008).

[8] L. Lindsay, D. A. Broido and N. Mingo, "Flexural phonons and thermal transport in graphene", *Phys. Rev. B*, vol. 82, 115427(1)-(6), (2010).

[9] L. Lindsay, D. A. Broido and Natalio Mingo, "Flexural phonons and thermal transport in multilayer graphene and graphite", *Phys. Rev. B*, vol. 83, pp. 235428 (1)-(5) (2011).

[10] X. Xu, Y. Wang, K. Zhang, X. Zhao, S. Bae, M. Heinrich, C. T. Bui, R. Xie, J. T. L. Thong, B. H. Hong, K. P. Loh, B. Li and B. Ozyilmaz, "Phonon transport in suspended single layer graphene", Preprint at <http://arxiv.org/abs/1012.2937>, pp.1-4, (2010).

[11] The expressions of κ for various cases are derived in R. Verma, S. Bhattacharya and S. Mahapatra, "Physics based thermal conductivity model for single layer graphene", *IOP: Semicond. Sc. Technol.*, Vol. 28, pp. 015009 (1)-(6), 2013.

[12] The expressions of $R(T)$ are derived in R. Verma, S. Bhattacharya and S. Mahapatra, 'Physics-Based Solution for Electrical Resistance of Graphene under Self-Heating Effect', *IEEE Trans. Electron Dev.*, vol. 60, pp. 502-505, (2013).

[13] R. Verma, S. Bhattacharya and S. Mahapatra, "Analytical Solution of Joule-Heating equation for Metallic Single-Walled Carbon Nanotube Interconnects", *IEEE Trans. Electron Dev.*, vol. 58, pp. 3991-3996, (2011).

[14] E. V. Castro, H. Ochoa, M. I. Katsnelson, R. V. Gorbachev, D. C. Elias, K. S. Novoselov, A. K. Geim and F. Guinea, "Limits on charge carrier mobility in suspended graphene due to flexural phonons", *Phys. Rev. Lett.*, 105, 266601(1)-(4), (2010).

[15] E. Mariani and F. v. Oppen, "Flexural Phonons in Free-Standing Graphene", *Phys. Rev. Lett.*, vol.100, pp. 076801(1)-(4), (2008).

[16] K.V. Zakharchenko, M.I. Katsnelson, A. Fasolino, "Finite Temperature Lattice Properties of Graphene beyond the Quasiharmonic Approximation", *Phys. Rev. Lett.*, vol. 102, pp. 046808(1)-(4), (2009).

[17] K. I. Bolotin, K. J. Sikes, J. Hone, H. L. Stormer and P. Kim, "Temperature-dependent transport in suspended graphene", *Phys. Rev. Lett.*, vol. 101, pp. 096802(1)-(4), (2008).

[18] M. T. Pettes, I. Jo, Z. Yao and L. Shi, "Influence of polymeric residue on the thermal conductivity of suspended bi-layer graphene", *Nano Lett.*, vol. 11, pp. 1195-1200, (2011).